VOL. 14, NO. 3, FEBRUARY2019 ISSN 1819-6608
ARPN Journal of Engineering and Applied Sciences

www.arpnjournals.com

PERFORMING LABORATORY STUDY ON THE IMPACT OF CHANGE IN THE ANGLE OF THE FIBRE-REINFORCED PLASTIC(FRP) SCREW FIBERS ON THE COMPRESSIVE BEHAVIOR OF THE ENCLOSED CONCRETE CYLINDERS

Azhar Ayad Jaafar[1], Mohammad Reza Tavakolizadeh[2], Douread Raheem Hassen[1], Thaer Matlab Mezher[3] and Alyaa Abdulrazzaq Azeez[1]
[1]Ministry of Education, Iraq
[2]Department of Civil Engineering, Ferdowsi University of Mashhad, Iran
[3]University of Kufa, Ministry of Higher Education, Iraq
E-Mail: dou_444@yahoo.com

ABSTRACT

The applications of FRP-based polymers for improving concrete structures have been significantly growing during the recent years. The main cause for the aforesaid extension deals with the requirement for extending the life of the infrastructure and improving the infrastructure in all parts of the world. High hardness, low weight, corrosion resistance, easy and quick installation, greater flexibility in design, lower total cost (including time, materials and performance) than steel sheets are the important features of FRP. The efficiency of the FRP enclosure function deals with the compressive strength of the concrete feature, the material and thickness of the pin and the angle or direction of the fiber. The axial behavior and bearing capacity of the columns are a function of the stress level of the aggregate conglomeration. The type of fiber, the number of ply layers, the fiber positioning angle and the compressive strength of the concrete are important in the column behavior. The parameters investigated and studied in the present research were investigated the impact of type of fibers including GFRP and CFRP, number of polychromatic layers, pinch angle, concrete compression strength of samples, including 3 resistances of 20, 35, 50 MPa, as well as the adhesion pattern of fibers. Considering the aforesaid cause and objective, 23 samples of unconventional concrete cylinders with a diameter of 200 mm and a height of 600 mm including 10 samples with a zero-degree fiber orientation, 10 samples with different fiber positioning angles and 3 control samples were tested for comparison. Following the rounded specimens' processing, they were subjected to a pure axial pressure test at a fixed rate of displacement through a hydraulic jack. The measured values in this work included axial stress, axial strain and lateral strain. Based on the results, the number of layers and its type bears a great impact on sample behavior. Based on the results, the amount of resistance, formability and absorbed energy of the samples increase with the polishing of the column. Plus the aforesaid, raising the angle of the fiber position relative to the horizon, results in decrease in the amount of resistance, absorbed energy, and formability.

Keywords: concrete, fiber-reinforced plastic (FRP), enclosure, axial behavior, fiber angle.

INTRODUCTION

In recent years, repair, refurbishment and reinforcement techniques for reinforced concrete columns have excessively been applied in the field of reinforced polymer fibers (FRP) due to their inherent qualities (high strength to weight ratio, high corrosion resistance and easy to install). It is applied in replacement for covering with steel. Many parameters affect the enclosure efficiency of concrete columns with FRP, including concrete strength, polymer fiber type, coating thickness, or number of FRP layers (strut stiffness) and the angle or direction of the fiber or the layer. Reinforcing concrete components with FRP composite materials is a relatively new method. FRP materials have good physical properties that can be characterized by high tensile strength and low thickness and weight. In concrete columns, the application of FRP, while increasing the shear capacity of the column, changes its rupture mode from shear to bending and raises the porosity considerably. The screw compression of the FRP fiber compression components raises their compressive strength. It also raises the form of the components by combining axial forces and bending forces. To enclose the concrete member, it is necessary to align the fiber alignment as far as possible perpendicular to the longitudinal axis of the member. In this situation, the circular fibers are similar to closed valves or steel helical silts. In calculating the axial compressive strength of a member, the contribution of the parallel fiber to its longitudinal direction should be ignored. When the pillar or compression member is subjected to seismic loads, the energy absorption capacity and the shape of the column are important. In this connection, the retrofitting or refinement of that member is carried out with increasing ductility, the disadvantages of this method are high cost, frailty behavior and its low resistance to fire [1]. A large number of studies are carried out on FRP recumbent columns under single-acting compressive loading, in which the layers have an angle of 0 ° with environmental direction, and a number of studies have been done with the insertion of fibers in a direction other than the circular direction. Kumutha et al. [2] studied the impact of the dimensions of polymer-reinforced fiber glass fiber reinforced polyester resin columns (GFRP). They studied three different dimensions of a/b=1, a/b=1.25, and a/b=1.66; where, "a" and "b" respectively are the length and width of the column. They consisted of nine

completely enclosed samples, which consisted of three control samples, until the moment of failure under the pressure of the pressure barrel. All samples had a fixed length and area of 750 mm and 15625 mm square, respectively. In most cases, the failure occurred near the corner points, due to the concentration of tension in these areas. The column with a ratio of 1.66 has resulted in the lowest values of the ultimate axial and lateral strain compared to the column with a ratio of 1.25. Mirmiran and Shahawy [3] performed experiments on FRP tubes filled with concrete at a diameter of 152.5 × 305 mm and under load-bearing area. E-glass fibers were orientated in a single direction with a ± 15 ° twist angle. The thickness of the sweatshirts of 14, 10.6 layers was tested, while the wrapping angle was fixed. Their findings showed that increasing the thickness of the sweater, the strength and shape of the jacket also rose. Concerning all the aforesaid, their researches on a twisting angle without further discussion focused on this parameter. Rochette and Lobossiere [4] examined the impact of the layer thickness and the shape of the short column of the column on its resistance axially. The columns were square, circular, and rectangular. The layers had a 0 ° angle with a horizontal axis, except for a square specimen with a circular / angle (45°/0°) circumference. Their results showed that the enclosure improved the resistance of the short column to the load-bearing margin by 92%. The change in the number of layers of a square pillar with a carbon or Aramid improved the strength and deformation by increasing the number of layers. The column with the shape of the layer (ring / angle) showed a strange behavior. Although the maximum resistance of the 5-layer (ring / angle) enclosure increased compared to the 4-layer ring enclosure, its shape was decreased, the number of layers were chosen in a way that the total enclosure hardness of the 5 layers (ring / angle) was approximately equivalent to the 4-layer enclosure.

On the other hand, the confinement for the concrete column by other material that has good tensile strength give a good enhancement to increase axial load [5].

METHODS AND MATERIALS

In order to investigate the impact of FRP cores on the capacity of concrete columns and the impact of the number of layers in this research, 40 laboratory samples were constructed. Unassembled concrete pillars of 600 mm in diameter and 200 mm in diameter. Finally, 40 concrete columns were constructed, 23 tested (10 samples with FRP fibers in the peripheral direction, and 10 samples with a change in orientation of the FRP fibers with environmental permeability and 3 control samples). Making more specimens allowed the possibility of, if needed, damage to the samples and mistakes in experiments, a number of other concrete columns with the same specifications would be available. The specimens were subjected to the following conditions and tested:

1) FRP screw-type specimens in perpendicular direction
- Examples of 200 mm diameter and 600 mm high
- Compressive strength of concrete 50.35, 20 Mpa
- The modulus of FRP elasticity for (CFRP, GFRP) is 230,70 Gpa
- Material of Fibers
- The number of layers (three-layer thickness) of a single, double-layer, and three-layer.
- Fiber angle (zero degree)

2) Examples with FRP screws with different angles
- Examples of 200 mm diameter and 600 mm high
- Gas compression strength 35 Mpa
- Edge of 230 Gpa elasticity
  Carbon fiber is applied for the angle
- The number of layers (the thickness of the hinges) of a single layer with a different angle and a double layer with a transverse angle (crosswise). - 3, 5, 8, 10 and 15 degree fiber yarns.

The most important factor in this study was the impact of FRP screw angle for three factors (fiber genus, number of layers (pitch thickness) and compressive strength of concrete) with two modes:

- Impact of different types of compressive strength 20, 35, 50 Mpa
- The impact of the number of single, double, and triple fiber fabrics with a resistance of 35 Mpa.

The concrete applied in this study is of a conventional type. In Table-1, the specification of the materials applied in concrete is shown.

Table-1. Specifications of materials applied in concrete.

Components	**Specific gravity** (kg/m^3)	**Gravel size** (mm)
Type I Cement	3150	-
Coarse Grained (gravel)	2640	20
Fine Grained (sand)	2580	-
Water	1000	-

In this research, three types of compressive strength are considered and concrete mixing plan based on the PCA method will be applied. The concrete was of the usual type I Cement. Concrete mixing designs with a resistance of 50 MPa were different with 20 and 35 MPa concrete, in which micro-silica additives and super-lubricants were applied. Micro silica is applied in the brand name of Jacquaw and super lubricant from the brand chemistry of building with the number P10-3R. CFRP and GFRP sheets were applied to reinforce and twist the columns. During the installation of CFRP and GFRP, the CFRP and GFRP cores were applied to strengthen the cylindrical specimens made of amber and hardener yellow to a yellowish transparent liquid, weighing 0.58: 1. In order to increase the precision of the test for the uniformity of concrete production, a total of 15 PVC

cylindrical moldings with a diameter of 200 mm and a height of 600 mm were applied to cut the tubes to the desired length of the Farsi machine to allow the edges of the pipe to be perpendicular to it. For the floor of the mold, a MDF board was applied, on which the grooves were created at a depth of half the thickness of the wood and the diameter of the pipe was created by a CNC machine. Therefore, after insertion of the tube into the groove and attaching the tube to the MDF board, through the aquarium adhesive, the pipe axis was perpendicular to the surface of the MDF board. It should be noted that the four triangles of the same MDF board are perpendicular to the quadrilateral MDF board and with the pipe; therefore, we can be firmly convinced when pouring concrete.

RESULTS AND DISCUSSIONS

In Figure-1, the stress-strain diagram of the non-fibrous control samples is shown. In the S20WL0-0˚ sample, the shape of the sample is evident and the drop is also seen at the end of the loading. In the S35WL0-0˚ sample, this behavior is similar to the S20WL0-0˚ sample. However, the behavior of the sample is in the behavior of high-strength crumbly concrete in the S50WL0-0˚ sample.

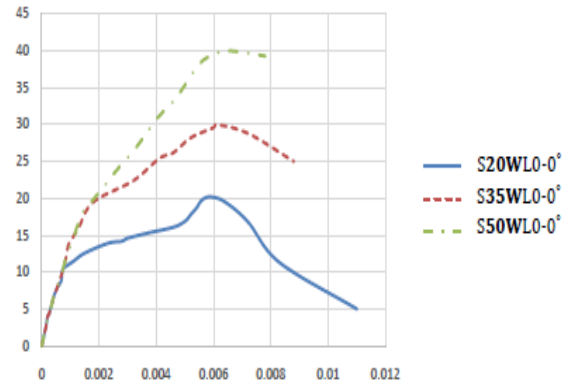

Figure-1. Stress-strain diagram of non-fiber control specimens.

In Figure-2, the stress-strain diagram is the axial and lateral strain of the carbon fiber stranded specimens with a single number with three strengths of 35, 20 and 50 Mpa, and the stress-strain diagrams of the glass-fiber samples are indicated in Figure-3.

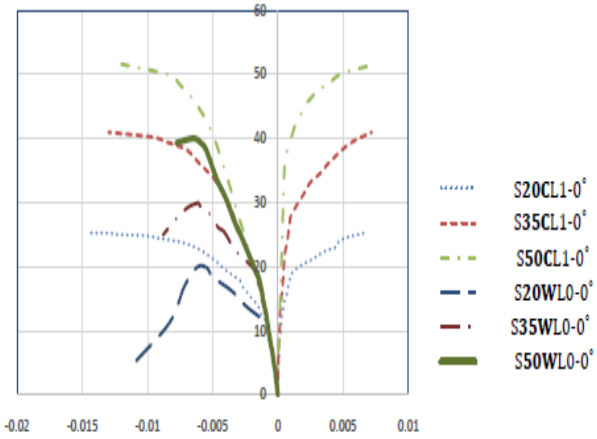

Figure-2. Stress-strain diagram of the axial and lateral strain of single-layer carbon fiber strands with different resistance.

Table-2. Mechanical specifications of carbon and single axis glass.

i	Name	Compressive strength (MPa)	fcc/fco	Maximum axial strain	Maximum lateral strain	Absorbed Energy (kN.m)	Ɛco / Ɛcc
1	S20GL1-0˚	22.3	1.10	0.013	0.0148	4.47	2.20
2	S35GL1-0˚	37	1.23	0.0125	0.0145	6.88	2.04
3	S50GL1-0˚	47	1.24	0.0115	0.013	7.47	1.76
4	S20CL1-0˚	25.3	1.25	0.0147	0.00675	5.84	2.49
5	S35CL1-0˚	41	1.32	0.013	0.0072	7.90	2.13
6	S50CL1-0˚	51.59	1.36	0.012	0.0075	8.45	1.93

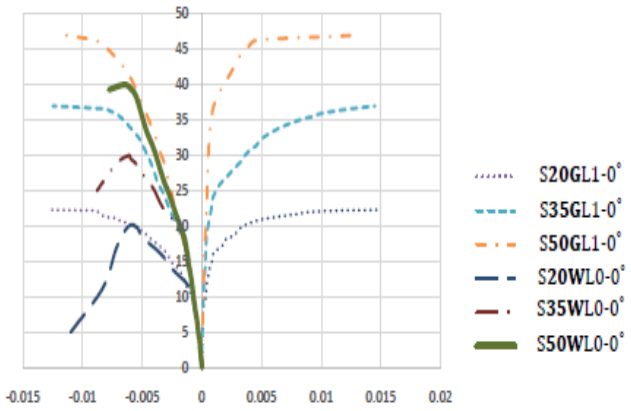

Figure-3. Stress and strain diagrams of the axial and lateral strain of single-layer glass fibers with different resistance.

As observed above, adding carbon fiber and glass to concrete columns raises the amount of resistance, absorbed energy and shape of the samples. The same trend is observed for the lateral strain of the samples. The permeability of the columns, with carbon fiber and glass fibers, is much higher than the non-fibrous specimens. The amount of lateral resistance of the samples is also increased due to the confinement of the fiber. Parameters of the amount of yield resistance, energy absorption and shape of the samples are given Table-2.

As you can see, the amount of resistivity, total absorbed energy, and the shape of carbon fiber samples are higher than that of glass fibers in the specified concrete strength. The absorbed carbon content of carbon samples ranges from about 13.2% to 30.7%, respectively, by resistivity of 20, 35 and 50 MPa, more than the absorbed energy of glass samples. The resistance of carbon specimens is more than that of glass because of the greater concentration of carbon fibers. The increase in the strength of the carbon fiber screw is about 13% instead of the glass hub. Due to the fact that the carbon fibers are more shaped than glass fibers, the shape of the carbon-fiber samples is more than the shape of the glass hollow glass samples. The shape of the carbon specimens is between 4.5 and 14% higher than those of glass. In all samples, the breakdown is due to the separation of carbon fiber and concrete glass. In the low resistors, the type of failure of the samples is generally shear and axially of a nearly soft type. But in a sample with a resistance of 50 MPa, the sample and fiber rupture occur suddenly. In Figure-4, the stress-strain diagram is the centrifugal and lateral strain of the carbon fiber stranded specimens with the number of 1, 2 and 3 layers with a resistance of 35 MPa, and in Figure-5, the stress-strain diagram of the axial and lateral strain of the glass-fibered specimens it has been shown with a number of different polygons.

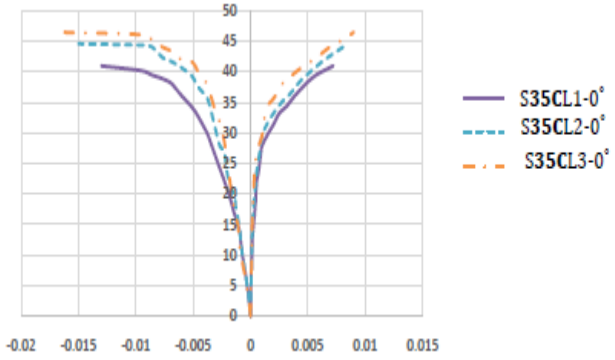

Figure-4. is the axial and lateral curvature of the curvature of multilayered carbon fiber columns with a resistance of 35 Mpa.

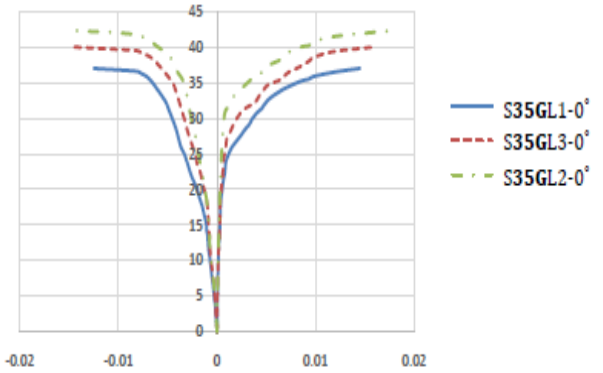

Figure-5. Axial and lateral strain curvature ofmultilayered glass fibers with a resistance of 35 Mpa.

In these samples, the compressive strength of concrete in samples is 35 MPa. As the addition of a number of carbon and glass layers has a significant impact on the axial behavior. Increased resistance and increased formability are found in all samples. The same increase is observed for samples absorbed by energy with a greater number of fibers. The same trend is observed for the lateral strain of the samples. By increasing the number of layers, the load-bearing load increased by the fibers due to the enclosure, and the value of the column's strength has also been increased. The amount of environmental resistance of the sample has also increased. In order to compare the impact of fiber type on the number of thumb screws for a resistance of 35 MPa, in Figure-6, a comparison between the types of fiber in different screws is shown for resistance to 35 Mpa.

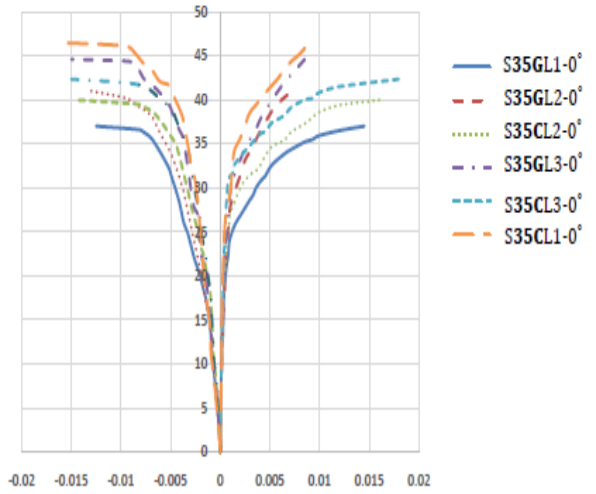

Figure-6. Stress and strain diagrams of the pivot and columnar glass and carbon fiber pillars with a resistance of 35 Mpa.

As indicated in Figure-6, the final axial stroke value of the glass fiber samples is lower than the final axial strain of the samples with carbon fiber. Subsequently, the formability of these samples is lower than that of carbon fiber. This reduced shape ability is due to the fractiousness of the glass fibers relative to the carbon fiber. In Figure-7, the stress-strain graphs of the axial and lateral strains of the single-layer carbon specimens, and in Figure-8, the stress-strain diagrams of the transverse carbon-carbon samples with different angles are compared with the environmental strain. In these samples, the strength of the concrete and the type of the hinges are the same and only the angle of positioning the fibers is different.

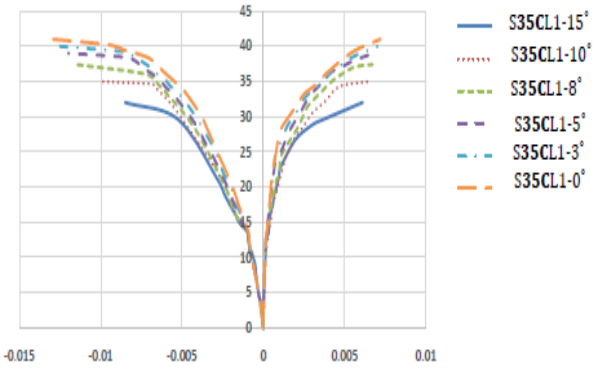

Figure-7. stress-strain graphs of the axial and lateral strains with different angles of the single-layercarbon specimens with a resistance of 35 Mpa.

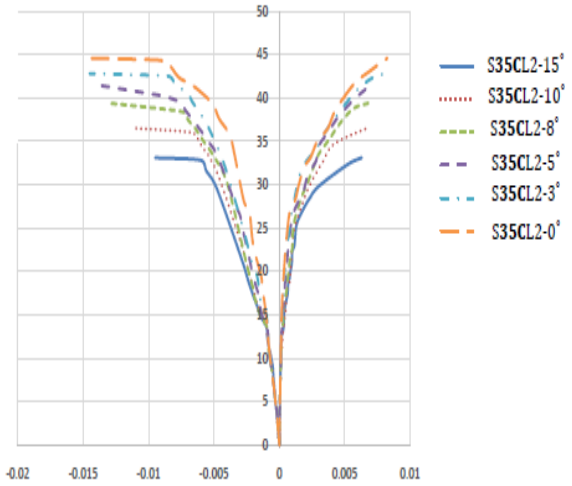

Figure-8. Stress-strain graphs of the axial and lateral strains with different angles of the cross two-layer carbon specimens with a resistance of 35 Mpa.

As shown in the above figures, in both single-layer and cross-sectional samples, by increasing the angle of position, the amount of resistance, absorbed energy, and formability decreases with respect to the horizon. The amount of absorbed energy decreases the shape; this is due to the axial strain with increasing angle of position relative to the lower horizon. By increasing the angle to the horizon, a percentage of the fibers are pressurized and, therefore, their contribution to bearing and hardness decreases. It can be seen that as the angle rose to the horizon, the resistance of the samples also decreases. Considering this behavior is also seen for the lateral stress-strain state. At 10 and 15 degrees, the difference between the graphs decreases. Table-3 shows the mechanical properties of these samples.

As can be seen, the amount of resistance decreases by increasing the angle of the fiber position relative to the horizon. As the axial force enters, the lateral strains increase on the basis of Poisson's principle and the tensile tension raises in the sample. This turbidity reduces the axial strength of the specimen. The lateral strains become more restrictive, the more powerful the specimen will tolerate. By wrapping the fibers around the specimen, the amount of enclosure is increased and the lateral strains and tensile cracks are reduced in the specimen. Because the most effective direction in the fibers, which produces the most resistance, is in the main direction of the fiber, it is better to wrap the fiber layers at zero angles to the horizon in the sample round.

CONCLUSIONS

In carbon fiber samples, the absorbed energy of carbon fiber samples ranges from about 13.2% to 30.7% more than the absorbed energy of glass fiber samples. The shape of the samples with carbon fiber is also more than the shape of glass it should be, regarding that carbon fiber samples are more shaped than glass fiber samples. The shape of the carbon fiber samples is between 4.5 and 14% higher than those of glass fiber. In samples with zero

degrees, in all samples, failure is due to the separation of the CFRP sheet and the GFRP from the concrete. In a sample with a resistivity of 50 MPa, a sample and fiber failure occurs suddenly. In the glass-fiber sample, this can be seen, but more carbon-fiber-shaped, for example. By increasing the number of layers from the one-bottle, the amount of absorbed energy of carbon fiber samples is approximately 51%, and with the same increase in glass-fiber samples, the absorbed energy raises by about 47%. Regarding that carbon fiber samples are more shaped than glass fiber samples, the increase in the number of layers of concrete samples also raises the shape of the samples with the carbon fiber screw more Gives The shape of the carbon fiber samples due to the increase in the number of layers is about 24.5% and the same amount in the glass samples is about 20.5%. In concrete samples with double-layer carbon fiber, the type of fracture of the sample is separated by the fiber from the surface of the concrete, but in a carbon-fiber sample with three layers of fibers, the specimen is discontinued as a fuser. This phenomenon may be due to the high adhesion between the adhesive and concrete layers. In this way, the amount of adhesive will reach the bottom and concrete levels and add to the adhesion strength of the sample, by increasing the fiber period. The type of failure of the samples is abrupt with the number of layers from a single glass fiber and broken by rupture of the fibers in small regions.

Table-3. Mechanical specifications of single and double ducts with various angles.

i	Name	Resistance (Mpa)	Maximum axial strain	Maximum lateral strain	Absorbed energy (kN.m)	ε_{co} / ε_{cc}
1	S35CL1-0˚	41	0.0130	0.0072	7.9	2.13
2	S35CL2-0˚	44.6	0.0150	0.0082	10.32	2.45
3	S35CL1-3˚	40	0.0125	0.0070	7.21	2.04
4	S35CL2-3˚	42.8	0.0145	0.0080	9.35	2.37
5	S35CL1-5˚	39	0.0120	0.0068	6.69	1.96
6	S35CL2-5˚	41.5	0.0140	0.0070	8.49	2.29
7	S35CL1-8˚	37.4	0.0115	0.0067	6.10	1.88
8	S35CL2-8˚	39.4	0.0130	0.0068	7.38	2.13
9	S35CL1-10˚	35	0.0100	0.0065	4.86	1.64
10	S35CL2-10˚	36.5	0.0110	0.0067	5.80	1.80
11	S35CL1-15˚	32	0.0085	0.0061	3.64	1.39
12	S35CL2-15˚	33.1	0.0095	0.0063	4.49	1.55

REFERENCES

[1] State Planning and Management Organization, Journal No. 525, Guide for the Methods and Approaches to improve Seismicity of Existing Buildings and Executive Details, 2010.

[2] Kumutha R. and Vaidyanathan M.S. Palanichamy. 2007. Behavior of reinforced concrete rectangular columns strengthened using GFRP. Cement & Concrete Composites.29: 609-615.

[3] Mirmiran A. and Shahawy M. 1997. Behavior of Concrete Columns Confined by Fiber Composites. J Struct Eng. 123: 583-590.

[4] Rochette P. and Labossiere P. 2000. Axial Testing of Rectangular Column Models Confined with Composites. J Compos Constr. 4: 129-136.

[5] Azeez A. A., Jamaluddin N., Abd Rahman N., Hassen D. R. and Attiyah A. N. 2018. Experimental and Analytical Study of PVC Confined Concrete Cylinders. Journal of Engineering and Applied Sciences. 13: 2145-2151.